PHYSICAL REVIEW B **80**, 140401(R) (2009)

Vortex oscillations induced by spin-polarized current in a magnetic nanopillar: Analytical versus micromagnetic calculations

A. V. Khvalkovskiy,[1,2,*] J. Grollier,[1] A. Dussaux,[1] Konstantin A. Zvezdin,[2,3] and V. Cros[1]
[1]*Unité Mixte de Physique CNRS/Thales and Université Paris Sud 11, 1 ave A. Fresnel, 91767 Palaiseau, France*
[2]*Istituto P.M. srl, via Cernaia 24, 10122 Torino, Italy*
[3]*A. M. Prokhorov General Physics Institute, RAS, Vavilova strasse 38, 119991 Moscow, Russia*
(Received 8 September 2009; published 2 October 2009)

We investigate the vortex excitations induced by a spin-polarized current in a magnetic nanopillar by means of micromagnetic simulations and analytical calculations. Damped motion, stationary vortex rotation and the switching of the vortex core are successively observed for increasing values of the current. We demonstrate that even for small amplitude of the vortex motion, the analytical description based on the classical Thiele approach can yield quantitatively and qualitatively unsound results. We show that the energy dissipation function, which is calculated respecting rotational motion of the vortex, can be used for qualitative analytical description of the system.

DOI: 10.1103/PhysRevB.80.140401 PACS number(s): 75.47.−m, 75.40.Gb, 85.75.−d

A magnetic vortex is a curling magnetization distribution, with the magnetization pointing perpendicular to the plane within the nanometer size vortex core. This unique magnetic object has attracted much attention recently because of the fundamental interest to specific properties of such a nanoscale spin structure. Gyrotropic modes of vortices in magnetic nanocylinders have been intensively studied theoretically[1] and experimentally.[2] Apart from their fundamental relevance, the unique properties of the vortices are of considerable practical interest for applications in magnetic memory and microwave technologies. In this view, the switching of the vortex core by magnetic field and spin-polarized current has been thoroughly studied.[3–6] More recently, sub-GHz dynamics of magnetic vortices induced by the spin-transfer effect observed in nanopillars and nanocontacts[7–9] have raised a strong interest. Indeed, the associated microwave emissions in such vortex-based spin-transfer nano-oscillators (STNOs) occur at low current densities, without external magnetic field, together with high powers and narrow linewidths (<1 MHz) comparatively to single-domain STNOs.

Traditionally, the analytical description of the vortex gyrotropic motion is based on the general approach for a translational motion of a magnetic soliton in an infinite media developed by Thiele.[10] This calculation consists in a convolution of the Landau-Lifshitz-Gilbert (LLG) equation with the magnetization distribution under a specific condition of a translational motion of the magnetization pattern. Eventually a single equation (often referred to as the Thiele equation) for the vortex core position **X** can be derived. The approach developed by Thiele to build his equation has been used for a long time to derive equations of vortex motion in many magnetic systems. In particular, it is often used to describe analytically the vortex oscillations induced by spin current[11–14] in magnetic nanodisks, in the "*current perpendicular to the plane*" (CPP) or "*current in the plane*" (CIP) configurations. Vortex dynamics in magnetic submicron disks cannot be considered as translational due to a strong deformation of the vortex structure by the edges.[15] Guslienko *et al.* demonstrated that this deformation should be taken into account in the calculation of the system energy.[1] However we show here that the impact of the spatial confinement on the vortex dynamics is much deeper. Our results demonstrate that, even if a proper model magnetization distribution is used, the Thiele approach applied for CPP nanodisks with a spin current can give rise to significant qualitative and quantitative errors. We suggest to use a different analytical technique to estimate the spin current-induced effects in such systems.

In our calculations we consider vortex motion in a vortex STNO. The system under study is sketched in the inset of Fig. 1. The nanopillar spin valve has a circular cross section. The reference layer is a fixed perpendicular polarizer, the polarization vector **p** is perpendicular to the plane, and, to be clear in our interpretations, we disregard the stray magnetic field emitted by it. The initial magnetization distribution in the free layer is a vortex; the magnetization within the vortex core is parallel to **p**. The current flow is assumed to be uniform in the pillar, with an axial symmetry of the current lines in the contact pads. The spin-transfer term[16] in the calculations is given by $(\sigma J/M_s)\mathbf{M}\times(\mathbf{M}\times\mathbf{p})$, J is the current density, **M** is the magnetization vector, M_s is the magnetization of saturation and σ represents the efficiency of the spin-

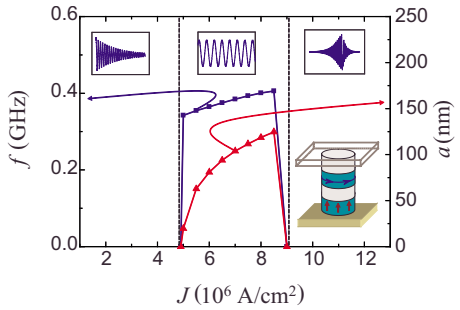

FIG. 1. (Color online) Steady vortex gyration induced by the spin-polarized current: frequency $f=\omega/2\pi$ (squares) and radius of the vortex core orbit a (triangles) as a function of the current density J (numerical simulations). Top insets: illustrations for the time evolution of the averaged projection of the free layer magnetization on the polar axis, for $J<J_{C1}$ (left), $J_{C1}<J<J_{C2}$ (center) and $J>J_{C2}$ (right), in arbitrary units. Bottom inset: sketch of the device geometry.

transfer torque: $\sigma=\hbar P/(2|e|LM_s)$, P is the spin polarization of the current, e is the charge of the electron, L is the sample thickness.

As a starting point for our analytical calculations, we use a shortened form of the Thiele equation as in Ref. 1 to account for the frequency of low-amplitude vortex oscillations in magnetic nanodisks,

$$\mathbf{G}\times\frac{d\mathbf{X}}{dt}-\frac{\partial W(\mathbf{X})}{\partial\mathbf{X}}=0. \tag{1}$$

Here the gyrovector $\mathbf{G}$ is given by

$$\mathbf{G}=-\frac{M_s}{\gamma}\int dV\sin\theta(\nabla\theta\times\nabla\varphi), \tag{2}$$

where γ is the gyromagnetic ratio, θ,φ are the magnetization angles. The integration in Eq. (2) is over the magnetic disk. $W(\mathbf{X})$ is the potential energy of the shifted vortex. Guslienko *et al.*[1] showed that an appropriate model magnetization distribution for a moving vortex is given by *the two-vortices ansatz* (TVA),

$$\varphi(\rho,\chi;a,\chi_v)=g_a(\rho,\chi-\chi_v)+\chi_v,$$

$$g_a(\rho,\chi)=\tan^{-1}\left(\frac{\rho\sin\chi}{\rho\cos\chi-a}\right)+\tan^{-1}\left(\frac{\rho\sin\chi}{\rho\cos\chi-R^2/a}\right)+C. \tag{3}$$

Here ρ,χ are polar coordinates in the disk plane, $a=|\mathbf{X}|$ is the vortex core displacement, (a,χ_v) is the position of the vortex core center, R is the radius of the dot and $C=\pi/2$ or $C=-\pi/2$ for different regions of the dot. The TVA [Eq. (3)] defines a spin structure that satisfies the magnetostatic boundary conditions, i.e., assumes zero magnetic charges on the side borders of the disk. The out-of-plane magnetization component $M_s\cos\theta$ can be described by a bell-shaped function, that is nonzero in the core region a few nanometers in diameter.[17] Using Eq. (1), hereafter we address analytically the vortex gyrotropic motion with a frequency ω and a small orbit radius a,

$$\dot{\mathbf{X}}=\omega\mathbf{e}_z\times\mathbf{X},\quad a\ll R. \tag{4}$$

It follows from Eq. (2) that the gyrovector is given by $\mathbf{G}=-G\mathbf{e}_z$, where $G=2\pi M_sL/\gamma$ is the gyroconstant.[1] At small current densities, the major contribution to the vortex energy $W(\mathbf{X})$ is the magnetostatic energy W_m, arising from the appearance of volume magnetic charges for a shifted vortex. It is given by $W_m(a)=\frac{20}{9}\pi M_s^2L^2a^2/R$.[1] Recent simulations have shown that the contribution of the Oersted magnetic field generated by the current can be very important.[18] Therefore we also calculate the energy contribution W_{Oe} due to the Oersted field. W_{Oe} is given by integration of the energy density $-\mathbf{H_{Oe}}(\mathbf{r})\cdot\mathbf{M}(\mathbf{r},\mathbf{X})$ over the volume, where $\mathbf{H_{Oe}}(\mathbf{r})$ is the Oersted field distribution at a given point $\mathbf{r}$. The integration yields $W_{Oe}(a)=1.70\pi LRM_sJa^2/c$.[19] Summing up these two contributions and using Eqs. (1) and (4), one gets the analytical prediction for the vortex frequency,

$$\omega=\omega_0^m+\omega_{Oe}J, \tag{5}$$

where $\omega_0^m=\frac{20}{9}\gamma M_sL/R$ and $\omega_{Oe}=1.70\gamma R/c$, c is the speed of light.

At the next step we calculate the energy dissipation function $\dot{W}=\int(\frac{\delta E}{\delta\theta}\dot{\theta}+\frac{\delta E}{\delta\varphi}\dot{\varphi})dV$,[11] which will give us the critical current to excite the vortex oscillations. Taking $\frac{\delta E}{\delta\theta}$ and $\frac{\delta E}{\delta\varphi}$ from the LLG equation, one finds

$$\dot{W}=-\frac{M_s}{\gamma}\int dV[\alpha(\dot{\theta}^2+\sin^2\theta\dot{\varphi}^2)-\gamma\sigma J\sin^2\theta\dot{\varphi}], \tag{6}$$

α is the Gilbert damping. The term proportional to α represents the natural damping; the second term is due to the spin torque, it can be positive or negative according to the current sign. For a steady motion, the energy is conserved ($\dot{W}=0$); thus after some algebra, one can find from Eqs. (4) and (6),

$$2\alpha\eta\omega=\gamma\sigma J, \tag{7}$$

where $\eta=\frac{1}{2}\ln(R/2l_e)+\frac{3}{8}$, the exchange length is $l_e=\sqrt{A/2\pi M_s^2}$, A is the exchange stiffness. From Eqs. (5) and (7) we get an expression for the critical value J_{C1} of the current density to excite the vortex oscillations,

$$J_{C1}=\frac{\alpha\eta\omega_0^m}{\gamma\sigma/2-\alpha\eta\omega_{Oe}}. \tag{8}$$

A different prediction follows from the Thiele approach. The Thiele equation that takes into account the damping and the spin-transfer effect in the CPP configuration is given by[11,12]

$$\mathbf{G}\times\frac{d\mathbf{X}}{dt}-\frac{\partial W}{\partial\mathbf{X}}-\hat{D}\frac{d\mathbf{X}}{dt}+\mathbf{F}_{ST}=0, \tag{9}$$

where the spin-transfer force $\mathbf{F}_{ST}$ is

$$\mathbf{F}_{ST}=M_sL\int(\sigma J)\nabla\varphi\sin^2\theta dV \tag{10}$$

(a different expression for $\mathbf{F}_{ST}$ has been derived for CIP systems[13]). $\hat{D}$ is the damping tensor,

$$\hat{D}=-\frac{\alpha M_s}{\gamma}\int dV[\nabla\theta\nabla\theta+\sin^2\theta\nabla\varphi\nabla\varphi]. \tag{11}$$

For circular dots, $\hat{D}=D\hat{E}$, where $\hat{E}$ is a unit tensor and the damping constant is $D=\alpha\eta' G$.[20] The factor η' and the previously introduced η define the same quantity even if they are given by different expressions, as we discuss below. Calculation of the spin-transfer force by Eq. (10) for the TVA yields $\mathbf{F}_{ST}=2\pi M_sL\sigma Ja\mathbf{e}_\chi$.[11,12] For a steady gyrotropic motion, the third and the last terms of Eq. (9) are perpendicular to the first and the second terms. Therefore the frequency of the vortex motion, given by Eq. (1), is not affected by the supplementary terms of Eq. (9); instead, they define the amplitude of the vortex motion.[11]

For the steady motion, the damping term is balanced by $\mathbf{F}_{ST}$; thus one gets

$$\alpha\eta'\omega = \gamma\sigma J. \quad (12)$$

Comparing this to Eq. (7), we see that Eq. (12) yields about a twice smaller value of the first critical current J_{C1}.

The reason of this difference is related to the breakdown of the assumption of a translational motion for the vortex, thus of the basic underlying assumption for the Thiele approach. Indeed, the *derivation* of the terms $\mathbf{G}$, $\mathbf{F}_{ST}$, and $\hat{D}$ [Eqs. (2), (10), and (11)] essentially uses the following feature of the translational motion of a magnetic soliton: $\dot{\mathbf{M}}=-(\dot{\mathbf{X}},\nabla)\mathbf{M}$.[11] However, one finds from the TVA and the micromagnetic simulations, that the magnetic moments at the disk side border are aligned along the border line; these moments stay still when the vortex is moving. Thus the left-hand side of this expression vanishes for the regions close to the disk boundary. However the right-hand side has a finite value in these regions due to nonvanishing $\nabla\mathbf{M}$. $\mathbf{F}_{ST}$ is very sensitive to this discrepancy: integration over inner regions of the disk in Eq. (10) shows that about a half of the magnitude of $\mathbf{F}_{ST}$ originates from the boundary regions of the disk. That is in contrast to the gyrovector $\mathbf{G}$, which magnitude comes from the vicinity of the vortex core, where the discrepancy is negligible; to some extent, the same conclusion holds for the damping term $\hat{D}$ at $a \ll R$.

Recently, a generalization of the Thiele approach has been developed.[21] For a constrained vortex it allows deriving a generalized Thiele equation that has the same structure as Eq. (9). By treating Eq. (9) in this sense and comparing it to our results,[22] we find that the proper expression for the spin-transfer force and for the damping constant for our system are correspondingly $\mathbf{F}_{ST}=\pi M_s L\sigma J a\mathbf{e}_\chi$ and $D=\alpha\eta G$.

We now compare our analytical results to numerical micromagnetic simulations. In the simulations a nanopillar 300 nm in diameter is considered. The free layer is 10 nm thick and has the following magnetic parameters: $M_s=800$ emu/cm^3, $A=1.3\times10^{-6}$ erg/cm, and $\alpha=0.01$ (values for NiFe). We use a two-dimensional mesh with in-plane cell size 1.5×1.5 nm^2. The polarization is taken to be $P=0.2$. The micromagnetic simulations are performed by numerical integration of the LLG equation using our micromagnetic code based on the forth order Runge-Kutta method with an adaptive time-step control for the time integration.

We observe vortex excitations only for positive current, which is defined as a flow of electrons from the free layer to the polarizer. The vortex motion is damped for small current densities $J \le J_{C1}$, where the first critical current density $J_{C1}=4.9\times10^6$ A/cm^2. For larger currents, after some transitional period, the vortex is gyrating on a steady circular orbit. Interestingly, J_{C1} is about one order of magnitude less than the critical current density for excitation of magnetization oscillations in nanopillar STNOs with nominally uniform free magnetic layer.[23,24] The values of J for which the steady vortex oscillations are observed, are limited by the second critical current value $J_{C2}=9.0\times10^6$ A/cm^2. For $J \ge J_{C2}$, on reaching a critical orbit, the core of the vortex is reversed. The details of this process: appearance of a vortex with opposite polarity and an antivortex, annihilation of the latter with the original vortex, essentially reproduce the previous findings for the vortex core switching by the field or current.[4,5,12] After the reversal of the core, the direction of the vortex gyration is changed and the vortex oscillations are damped.

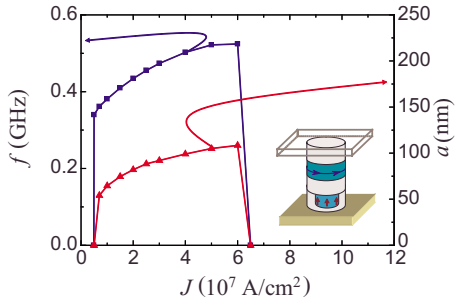

FIG. 2. (Color online) Numerical result for the constrained polarizer, in the notations of Fig. 1. Inset: sketch of the device geometry.

For each point within $J_{C1}<J<J_{C2}$, the vortex motion is simulated for 100 ns after reaching a stationary orbit. The vortex frequencies extracted from these simulations together with the radius of the oscillation orbit are presented in Fig. 1. On increasing J, the oscillation frequency increases ranging from 0.34 to 0.41 GHz. The radius of the orbit increases with the current as well, reaching 125 nm at $J=8.5\times10^6$ A/cm^2.

Analytical prediction for the vortex frequency at $J=J_{C1}$, given by Eq. (5), is $f=0.36$ GHz that is in a good correspondence to the simulation results $f=0.34$ GHz. This agreement (similar to that found in Ref. 1) owes to the fact that the gyrovector $\mathbf{G}$ and the energy derivative $\partial W/\partial\mathbf{X}$ are not sensitive to the violation of the assumption of the translational motion. The factor η for our system can be extracted using additional simulations. We find that if the current is switched off, the vortex motion is a gyration with the orbit damped in time as $a\propto\exp(-t/\tau)$, τ is a time constant. On the other hand, it follows from Eqs. (4) and (6) that at zero current $a\propto\exp(-\alpha\eta\omega t)$. Comparing this to the numerical results, we find $\eta=\eta'=1.65$ (Ref. 25) (in good agreement with the analytical prediction $\eta=1.71$).

Taking η and f from the simulations, we find from Eq. (7) that the analytical prediction $J_{C1}=4.5\times10^6$ A/cm^2 is in good agreement with the numerical result. The result of the Thiele approach [Eq. (12)] is $J_{C1}=2.3\times10^6$ A/cm^2, that illustrates our statement of its imperfection to account for the vortex motion in CPP nanopillars.

We demonstrate the deficiency of the Thiele approach in a different way. We perform simulations for a configuration that we call constrained polarizer for which the current polarization P equals 0.2 for $\rho\le50$ nm and $P=0$, hence, $\sigma=0$ for larger ρ. Thus for this structure the current does not excite the regions close to the disk border, in contrast to the case of the uniform polarizer. The resulted dependences $f(J)$ and $a(J)$ are presented in Fig. 2. We find for this configuration that $J_{C1}=(4.9\pm0.1)\times10^6$ A/cm^2 equals the critical current for a uniform polarizer. This is in perfect agreement with the analytical result obtained by considering the dissipation. Indeed, Eq. (6) gives equal results, hence equal values of J_{C1}, for both configurations at $a \ll R$.

The prediction of the Thiele approach for a constrained

polarizer is that the magnitude of the spin-transfer force $\mathbf{F}_{ST}$ [Eq. (10)] is a factor 1.8 less than that for a uniform polarizer. Accordingly, the value of J_{C1} in the two configurations differs at about the same factor, in contradiction to the numerical results. Thus we demonstrate that the Thiele approach can give rise to not only quantitative, but also qualitative disagreements.

Dependencies of the vortex frequency and orbit on the current for $J_{C1}<J<J_{C2}$ can also be treated analytically by taking into account higher-order terms in $W(a)$ and $\dot{W}(a)$. This study goes beyond the scope of this Rapid Communication and its results will be presented elsewhere. However we note that the most important among the higher-order terms is that of the damping parameter η, which appears to be a strong function of the vortex displacement. Another important nonlinear contribution owes to the magnetostatic energy.[11] These facts appear to be sufficient to get a qualitative understanding of $f(J)$ and $a(J)$ functions presented in Figs. 1 and 2.

Simulation results for the constrained polarizer contain other remarkable facts. We see that the second critical current $J_{C2}=6.5\times10^7$ A/cm^2 is by a factor of about 7 larger that J_{C2} for a uniform polarizer. The oscillation orbit gradually increases with the current reaching $a=108$ nm at $J=J_{C2}$. The oscillation frequency starts at $f=0.34$ GHz at J_{C1} like for a uniform polarizer but reaches a larger frequency $f=0.52$ GHz at $J=J_{C2}$.

It has been predicted that the vortex core is reversed if its velocity reaches a critical value v_{crit} that is about 340 m/s for permalloy independently of the device design.[6] Our simulation results are 320 m/s for the uniform polarizer and 350 m/s for the constrained polarizer in nice agreement with this prediction. A small difference between the values is presumably due to a different extent of the vortex deformation at critical orbits. The value of v_{crit} together with the dependencies of $f(J)$ and $a(J)$ define the value of the second critical current J_{C2}. As for the constrained polarizer $f(J)$ and $a(J)$ are much less steep functions than those for the uniform polarizer, J_{C2} in the former is substantially larger than in the latter. Larger frequencies at a given orbit, found for the constrained polarizer, are related to the strong influence of the Oersted field. These facts make this configuration promising for applications. It can be implemented by reducing the polarizer dimensions or simply by using a point-contact technique.

In conclusion, we demonstrate that the Thiele approach can fail to give a proper analytical description for the vortex motion in the CPP magnetic nanopillars due to the imperfection of the underlying assumption of the translational motion of the vortex. Instead, the analytical approach, which is based on the calculation of the energy dissipation and respects the rotational vortex motion, has shown to be in good agreement with the numerical results. Our calculations demonstrate that vortex-based STNOs can potentially have very low values of J_{C1}, large values of J_{C2} and operate at zero external magnetic field. This makes them promising candidates for future microwave technology applications.

The work is supported by the EU project MASTER (Project No. NMPFP7 212257) and RFBR (Grants No. 09-02-01423 and No. 08-02-90495).

*Corresponding author. On leave from the A. M. Prokhorov General Physics Institute of RAS, Moscow, Russia. khvalkov@fpl.gpi.ru

[1] K. Yu. Guslienko *et al.*, J. Appl. Phys. **91**, 8037 (2002).
[2] J. P. Park *et al.*, Phys. Rev. B **67**, 020403(R) (2003).
[3] B. Van Waeyenberge *et al.*, Nature (London) **444**, 461 (2006).
[4] R. Hertel *et al.*, Phys. Rev. Lett. **98**, 117201 (2007).
[5] K. Yamada *et al.*, Nature Mater. **6**, 270 (2007).
[6] K. Yu. Guslienko *et al.*, Phys. Rev. Lett. **100**, 027203 (2008).
[7] V. S. Pribiag *et al.*, Nat. Phys. **3**, 498 (2007).
[8] M. R. Pufall *et al.*, Phys. Rev. B **75**, 140404(R) (2007).
[9] Q. Mistral *et al.*, Phys. Rev. Lett. **100**, 257201 (2008).
[10] A. A. Thiele, Phys. Rev. Lett. **30**, 230 (1973); D. L. Huber, Phys. Rev. B **26**, 3758 (1982).
[11] B. A. Ivanov and C. E. Zaspel, Phys. Rev. Lett. **99**, 247208 (2007).
[12] Y. Liu *et al.*, Appl. Phys. Lett. **91**, 242501 (2007).
[13] A. Thiaville *et al.*, Europhys. Lett. **69**, 990 (2005).
[14] B. Krüger *et al.*, Phys. Rev. B **76**, 224426 (2007).
[15] K. L. Metlov and K. Yu. Guslienko, J. Magn. Magn. Mater. **242-245**, 1015 (2002).
[16] J. Slonczewski, J. Magn. Magn. Mater. **159**, L1 (1996).
[17] N. A. Usov and S. E. Peschany, J. Magn. Magn. Mater. **118**, L290 (1993).
[18] Y.-S. Choi *et al.*, Appl. Phys. Lett. **93**, 182508 (2008).
[19] The details of this calculation and verification will be given in a forthcoming publication. We note that for $J\leq10^7$ A/cm^2 the contribution of W_{Oe} to the total density is relatively small (1–10 %); however it can become predominant for larger J.
[20] K. Yu. Guslienko, Appl. Phys. Lett. **89**, 022510 (2006).
[21] O. A. Tretiakov *et al.*, Phys. Rev. Lett. **100**, 127204 (2008).
[22] The core of the approach of Ref. 21 is the calculation of generalized forces acting on a soliton. This is the key difference to our approach, which is based on the calculation of the system energy dissipation. In terms of generality and validity these two approaches are equivalent.
[23] S. I. Kiselev *et al.*, Nature (London) **425**, 380 (2003).
[24] This fact, which makes vortex nanopillar STNOs very promising for applications, is explained by the general statement that the critical magnitude of excitation scales with the energy of the excited mode. For a vortex STNOs, this statement is illustrated by our expression [Eq. (8)] and by earlier findings based on the Thiele approach (Ref. 11). A similar expression for uniform nanopillar STNOs is derived by A. N. Slavin and V. S. Tiberkevich, Phys. Rev. B **72**, 094428 (2005). As the frequencies of the excitations differ by about an order of magnitude, the critical current densities also differ by approximately the same factor.
[25] From Eq. (9) it follows $a\propto\exp(-\alpha\eta'\omega t)$ at $J=0$. Therefore η and η' are equivalent to each other; correspondingly, the simulations give a single value for η and η'.